Trop J Nat Prod Res, September 2025; 9(9): 4400 - 4417

ISSN 2616-0684 (Print)
ISSN 2616-0692 (Electronic)

Tropical Journal of Natural Product Research

Available online at https://www.tjnpr.org

Original Research Article

In Silico Molecular Docking Of Beta-Sitosterol and Astaxanthin into Cyclooxygenase Enzymes

Aqilatul R. A. Rahim[1], Muhammad I. Bashir[1]*, Zalina Zahari[1], Umar I. Ibrahim[1], Nureen F. M. Soufi[1], Nur I. Rosli[1], Mohamad H. N. Zainuddin[1]

[1]*Faculty of Pharmacy, Universiti Sultan Zainal Abidin, Besut Campus, Besut, Terengganu, Malaysia*

ARTICLE INFO

Article history:
Received 06 July 2025
Revised 18 August 2025
Accepted 21 August 2025
Published online 01 October 2025

ABSTRACT

Cyclooxygenase enzymes, mainly COX-1 and COX-2, have been shown to contribute to the regulation of inflammation, pain, and physiological homeostasis, positioning them as critical targets for the development of novel anti-inflammatory therapies. Although NSAIDs have proven their efficacy in COX inhibition, their adverse effects have limited their use, highlighting a research gap that necessitates further exploration of natural compounds, such as beta-sitosterol (BS) and astaxanthin (AXT), as potentially safer, selective COX modulators. This study aimed to explore the potential synergistic effects of BS-AXT combination in modulating COX enzymes through molecular docking to discover their combined activity as safer, natural anti-inflammatory agents. Docking results revealed that the BS-AXT combination significantly enhanced the binding affinity of BS to COX-2, improving from -7.5424 kcal/mol (alone) to -9.2033 kcal/mol in the combination form, indicating a potential synergistic interaction. Consistent with previous docking studies, BS and AXT demonstrated similar binding behaviors, dominated by hydrophobic interactions, particularly with key nonpolar residues within the COX-2 active site. In conclusion, the docking results suggest that the BS-AXT combination could be a natural COX-2 selective inhibitor, supporting the need for further studies to confirm its effectiveness and safety.

Keywords: Cyclooxygenase enzymes, Beta-sitosterol, Astaxanthin, Molecular docking, Combination docking, Natural anti-inflammatory, Synergistic interactions, In-silico study

Introduction

Cyclooxygenase (COX) enzymes, especially COX-1 and COX-2 isoforms, have been contributing to the proinflammatory prostaglandins (PGs) synthesis from arachidonic acid, resulting in the pathogenesis of inflammation and pain.[1,2] Although COX-1 is expressed constitutively and involved in physiological processes such as gastric mucosa protective barrier and platelet function, inducible COX-2 is significantly upregulated in response to inflammation and in various cancers such as breast and colorectal cancers.[3,4] Excessive COX-2 activity promotes PG overproduction, resulting in chronic inflammation.[5] Conventional COX inhibitors, such as non-steroidal anti-inflammatory drugs (NSAIDs), are effective but frequently associated with undesirable effects, such as gastrointestinal irritation and cardiovascular issues, which has driven the search for safer, naturally derived alternatives.[6,7] Beta-sitosterol (BS), a phytosterol found in plant-based foods, exhibits anti-inflammatory and antioxidant properties through COX inhibition and modulation of oxidative stress markers.[8,9] Similarly, astaxanthin (AXT), a xanthophyll carotenoid derived from marine sources, particularly *Haematococcus pluvialis*, exhibits potent antioxidant activity and has shown inhibitory effects on COX-1 and COX-2 through *in silico* studies.[10,11]

*Corresponding author; Email: irfanbashir@unisza.edu.my
Tel: +601111643282

Citation: Aqila RAR, MI Bashir, Zahari Z, Umar II, Naureen FMS, Nurinsyrah MR, MHN Zainudin. *In silico* molecular docking of beta-sitosterol and astaxanthin into cyclooxygenase enzymes. Trop J Nat Prod Res. 2025; 9(9): 4400 – 4417 https://doi.org/10.26538/tjnpr/v9i9.40

Official Journal of Natural Product Research Group, Faculty of Pharmacy, University of Benin, Benin City, Nigeria.

Although both compounds have been shown to exhibit COX inhibition and promising anti-inflammatory effects, their combined efficacy has not yet been explored.

Given the potential complementary mechanisms of BS and AXT, which involve direct COX inhibition and attenuation of oxidative stress, this study aimed to evaluate the potential of BS and AXT, individually and in combination, as natural COX inhibitors, using molecular docking analysis. The interactions of these compounds with COX isoforms will also be compared to those of the standard COX inhibitors, ibuprofen and celecoxib. This investigation could shed light on the potential synergistic mechanism of the combination and its viability as a safer anti-inflammatory and analgesic strategy.

Materials and methods

Materials

The chemical structures of four ligands: Ibuprofen (CID: 3672), Celecoxib (CID: 2662), Beta-sitosterol (CID: 222284) and Astaxanthin (CID: 5281224), were retrieved from the PubChem database (https://pubchem.ncbi.nlm.nih.gov) in the Simplified Molecular Input Entry System (SMILES) format. The structures of the target proteins, COX-1 (PDB ID: 6Y3C) and COX-2 (PDB ID: 3LN1), were retrieved from the RCSB Protein Data Bank (https://www.rcsb.org) in the legacy PDB format.

Methods

Ligands and Proteins Preparation

All docking preparations and simulations were performed using Molecular Operating Environment (MOE) software version 2015.10. Ligands were constructed in 3D using the "Builder" module by inputting SMILES strings, followed by geometry optimization and assignment of partial charges.

The structures of the target proteins were prepared by removing unwanted molecules such as water molecules, ligands, and redundant

chains. Protonation states were adjusted using the Protonate 3D tool, and missing residues were corrected in Structure Preparation mode. The protein active sites were identified using the "Site Finder" function and dummy atoms were placed to define the binding pocket for docking.

Molecular Docking

Ligands were docked into both COX isoform active sites using the MOE Dock mode. The docking process involved rigid receptor-flexible ligand docking with the placement method set to "Triangle Matcher" and refinement using "Forcefield". The top scoring poses were ranked based on binding energy (S score) and Root Mean Square Deviation (RMSD), with poses showing RMSD < 2.0 Å were considered valid.[12,13]

For combination docking, we used the sequence docking technique instead of the merge docking technique to individually observe the binding energies of the ligand combinations. BS was first docked into the protein, followed by AXT. Both ligands were docked simultaneously at the same site to evaluate potential synergistic binding interactions. Each docking simulation was repeated in triplicate to ensure the consistency of the results.

Visualization and Interaction Analysis

Docking interaction analyses were carried out using the BIOVIA Discovery Studio Visualizer 2025. Ligand-receptor interactions were visualized in both 2D and 3D formats. Hydrogen bonds and hydrophobic interactions were assessed, and key residues were identified and labeled accordingly.[14,15]

Methods by Modules

Module 1: Ligands Preparation

The chemical structures of four ligands; Ibuprofen (CID: 3672), Celecoxib (CID: 2662), Beta Sitosterol (CID: 222284) and Astaxanthin (CID: 5281224) were retrieved from the PubChem Database (https://pubchem.ncbi.nlm.nih.gov) in the Simplified Molecular Line Entry System (SMILES) format. These SMILES strings were used to generate three-dimensional (3D) structures in Molecular Operating Environment (MOE) software version 2015.10.

In the MOE, the ligands were constructed using the "Builder" module by inputting SMILES strings. Each structure was minimized in energy and prepared by applying geometry optimization and partial charge calculations via the "Compute > Prepare > Partial Charges" function. This process ensures proper electron distribution across atoms, which is critical for accurate electrostatic and hydrogen bond interaction prediction during docking. The optimized ligands were saved in the "moe" format and imported into ligand database file "mdb" using the MOE Database Viewer. Each ligand was added as a new entry to facilitate the batch docking and further manipulation. This preparation process consistently applied to both individual and combination docking simulations, including the redocking validation.

Module 2: Protein Preparation

The structures of COX-1 (PDB ID: 6Y3C) and COX-2 (PDB ID: 3LN1) were downloaded from the RCSB Protein Data Bank (https://www.rcsb.org) in Legacy PDB format. These structures were selected on the basis of their resolution and relevance to NSAID binding. The protein files were loaded into MOE 2015.10.

Protein preparation involved the removal of all heteroatoms, including co-crystallized ligands, water molecules and redundant chain, retaining only chain A for COX-1 and COX-2 in protein sequence "SEQ" function. The "Structure Preparation" tool was used to correct missing atoms or residues and optimize protein geometry. Subsequently, the "Protonate 3D" function was applied to assign the correct protonation states at physiological pH, which ensured an appropriate charge distribution and hydrogen bonding during docking.

The binding site was identified using MOE's "Site Finder" function to detect potential ligand-binding pockets. Alpha spheres were initially used to define the cavities, and dummy atoms were placed at the predicted binding site to guide docking. The binding site was refined by setting visualization parameters ("Render: Alpha Centers > No Centers" and "Isolate: None > Atoms and Backbone") to enhance docking focus and computational efficiency. The prepared protein structures were saved in "moe" format for subsequent docking procedures

Module 3: Docking of Ligands on Proteins

The prepared proteins (COX-1 and COX-2 in "moe" format) were loaded into the MOE 2015.10. Docking simulations were initiated through the "Compute > Dock" function. The binding site was defined using previously applied dummy atoms. Under the "Site" section, "Ligand Atoms" was set to "Dummy Atoms" to restrict docking to the active site.

In the docking window, under the "Ligand" section, input was set to "MDB File" and the ligand database viewer file containing the prepared ligand was selected. The "Output" path was defined to save the docking results. Each ligand was docked individually to COX-1 and COX-2 using the Triangle Matcher placement method and Forcefield refinement.

Docking results were displayed in the database viewer, where poses were evaluated based on Root Mean Square Deviation (RMSD). Poses with the RMSD < 2.0 Å were considered valid, indicating that the predicted ligand orientation was close to the optimal native binding mode. Docking for each ligand was repeated three times to ensure consistency. The best pose with the lowest binding energy, marked by the "S" symbol, was saved for the visualization by selecting the pose, clicking "Keep" and exporting it in "Tripos MOL2" format as Ligand-Protein Docked Pose1".

Module 4: Ligand Combination Preparation

For combination docking, the database viewer files of beta-sitosterol (Ligand C) and astaxanthin (Ligand D) were first duplicated and opened in separate windows in MOE. Using Ligand C's database viewer, the molecular structure was copied using "Copy As > MOE". In the Ligand D's viewer, a new empty entry was created via "Edit > New > Entry" and the copied Ligand C structure was pasted into this field. Both ligand entries (C and D) were selected, and the combined database was saved using "File > Save As" and named "Ligand C-D Complex Database Viewer" in "mdb" format. This file enabled the sequential docking of both compounds at the same active site.

Module 5: Combinatorial Docking of Ligands

To perform sequence docking, the prepared protein file was reopened on MOE 2015.10. Docking was started via "Compute > Dock". The binding site was defined using "Dummy Atoms" under the "Site" section, as previously set during site identification. In the "Ligand" section, the input was changed to "MDB File" and the combination file "Ligand C-D Complex Database Viewer" was loaded. The "Output" path was selected and saved as "Ligand C-D Combination-Protein Docked". Docking was executed by clicking "Run".

The docking results for ligands C and D were analyzed individually. Poses with the RMSD < 2.0 Å were retained, and those with the lowest binding energy were selected as optimal. Each selected pose was kept in the active site using "Keep" for both ligands and the resulting complex was saved in "Tripos MOL2" format as "Ligand-Protein Co-docked Pose 1". This sequence docking allowed for the analysis of how each ligand contributed to the binding site, simulating potential synergistic effects.

Module 6: Visualization of Ligand-Protein Interactions

The ligand-protein complex interactions were analyzed using BIOVIA Discovery Studio Visualizer 2025. The docked "MOL2" files ("Ligand-Protein Docked Pose 1" and "Ligand-Protein Co-docked Pose 1") were opened using "File > Open".

For single docking visualization, 3D and 2D interaction maps were generated via "Receptor-Ligand Interactions > View Interactions". The "Ligand Interactions" and "Show 2D Diagram" options were used to display the binding residues and interaction types. Unfavorable interactions were removed by right-clicking the interaction, selecting "Display Style" and unticking the undesired categories. For the ligand celecoxib, which may have delocalized bonds, the "Chemistry > Bond > Localize Bonds" function was used to correct bond visualization.

For co-docking analysis, the same process was repeated using "Ligand-Protein Co-docked Pose 1". The interactions of each ligand

ISSN 2616-0684 (Print)
ISSN 2616-0692 (Electronic)

were viewed separately using the "Step Through Ligands" arrow tool. Interaction diagrams and binding site residues were labeled in the 3D viewer for a clearer presentation of the hydrophobic and hydrogen bonding patterns.

Results and discussions

This section presents the molecular docking results of ibuprofen (IB), celecoxib (CX), beta-sitosterol (BS), and astaxanthin (AXT), both individually and in combination, against both COX isoforms. Table 1 presents the results related to COX-1 whereas Table 2 presents results for COX-2. Ligand-protein interactions were analyzed using 2D interaction diagrams and 3D visualizations. Key binding residues, bond types, and binding affinities have been reported previously. IB demonstrated a binding energy of -6.3164 kcal/mol with COX-1, forming hydrogen bonds with HIS A:43 and LYS A:468. Meanwhile, hydrophobic interactions were observed with CYS A:36, A:41, A:47,

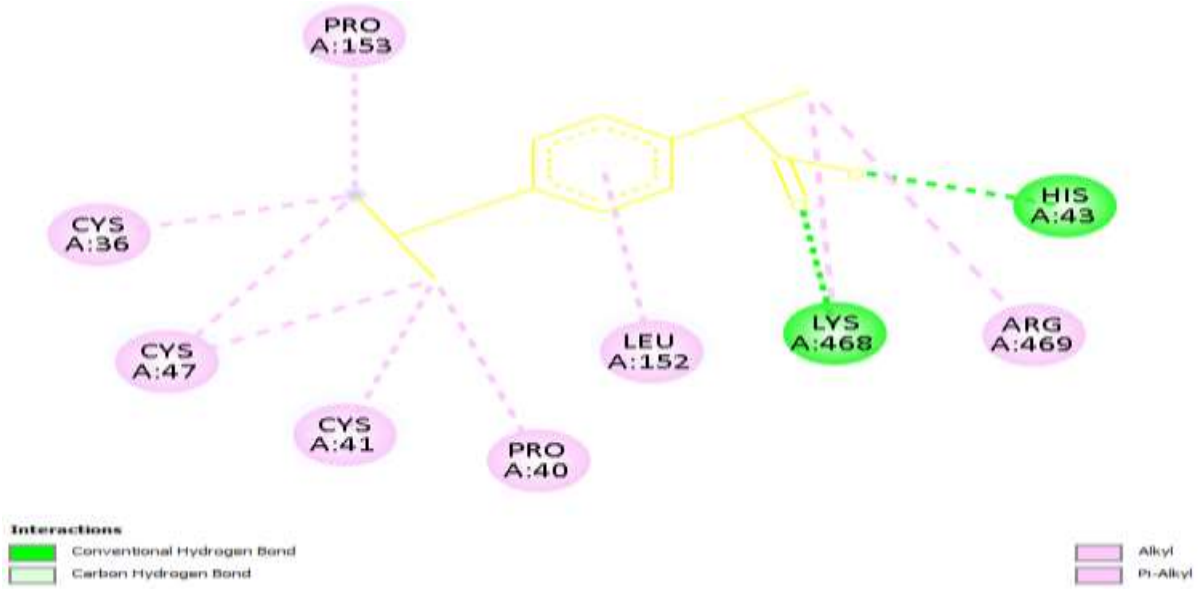

(a)

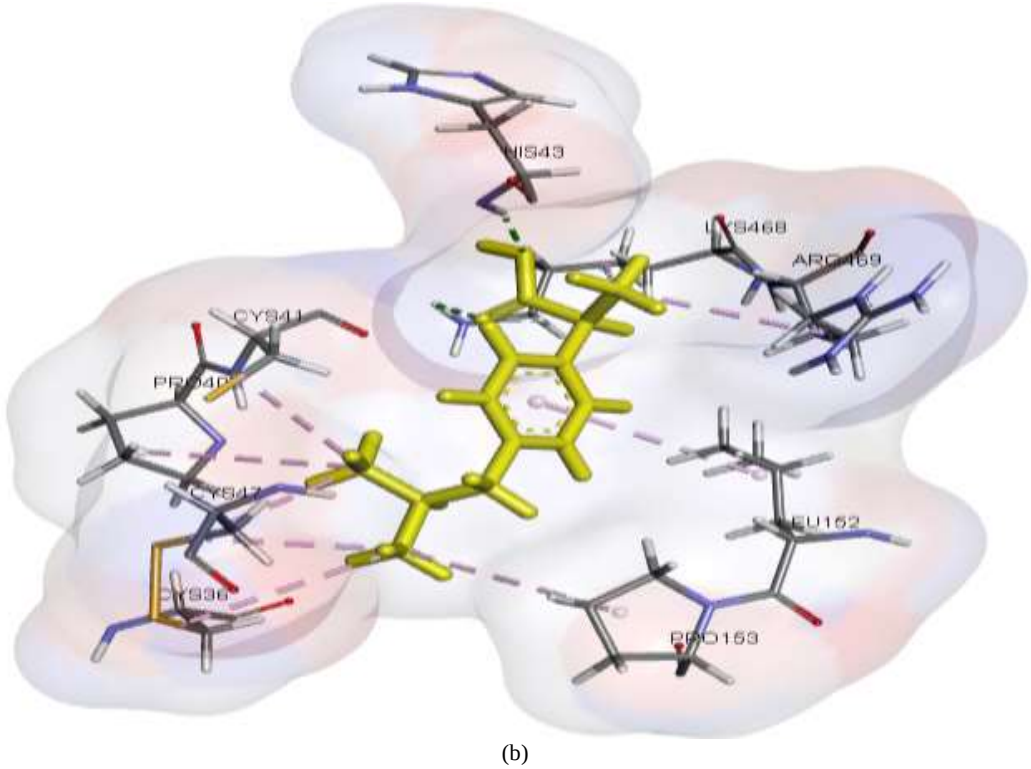

(b)

Figure 1 : Interaction of Ibuprofen with Cyclooxygenase-1 (COX-1). **(a)** 2D interaction showing the binding of ibuprofen to residues within the COX-1 active site. **(b)** 3D visualization of Ibuprofen spatial orientation and binding pocket topology within the active site.

PRO A:40, A:153, LEU A:152 and ARG A:469 (Figure 1). On COX-2, the binding energy was slightly lower (-6.2170 kcal/mol). Interactions included hydrogen bonds with ASN A:28 and GLN A:27, and hydrophobic contacts with CYS A:26, A:32, PRO A:25, A:139, LEU A:138, LYS A:454 and ARG A:455 (Figure 2). CX produced a binding energy of -7.4058 kcal/mol with COX-1 through conventional hydrogen bonds with GLU A:465, CYS A:41, and GLN A:42; carbon-hydrogen bonds with ARG A:469 and TYR A:130; and a halogen

ISSN 2616-0684 (Print)
ISSN 2616-0692 (Electronic)

(fluorine) bond with ILE A:151. Hydrophobic alkyl and pi-alkyl interactions were observed with CYS A:36, A:47, ILE A:46, LEU A:152, and PRO A:153 (Figure 3). With COX-2, CX bound more strongly (-7.5955 kcal/mol), forming hydrogen bonds with GLU A:451

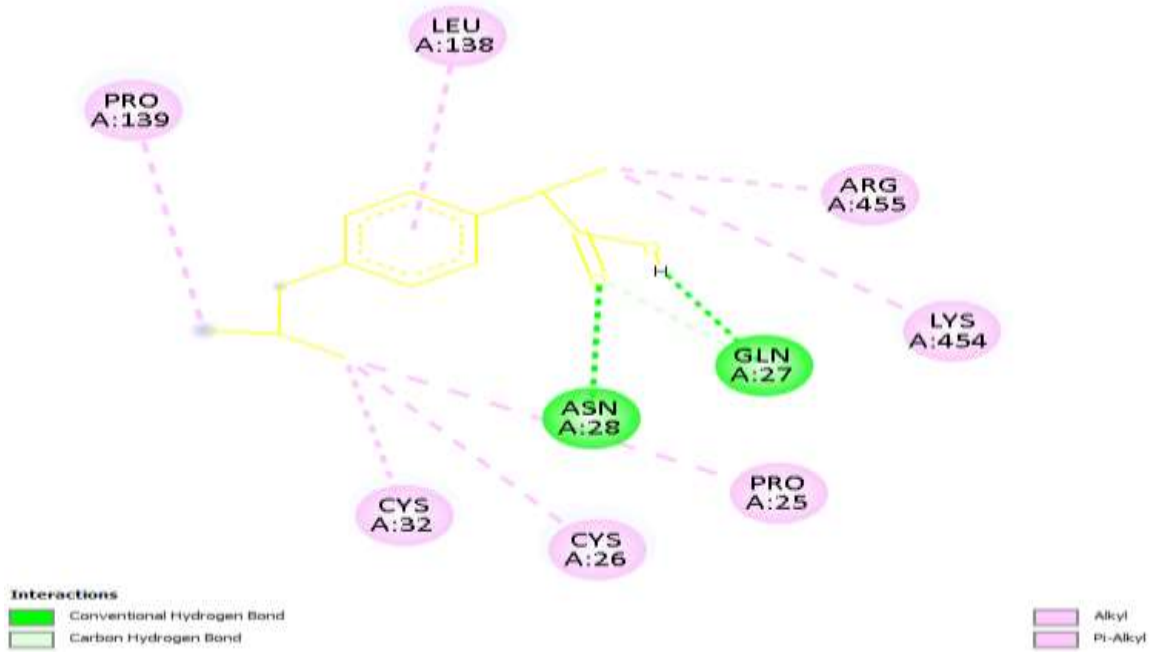

(a)

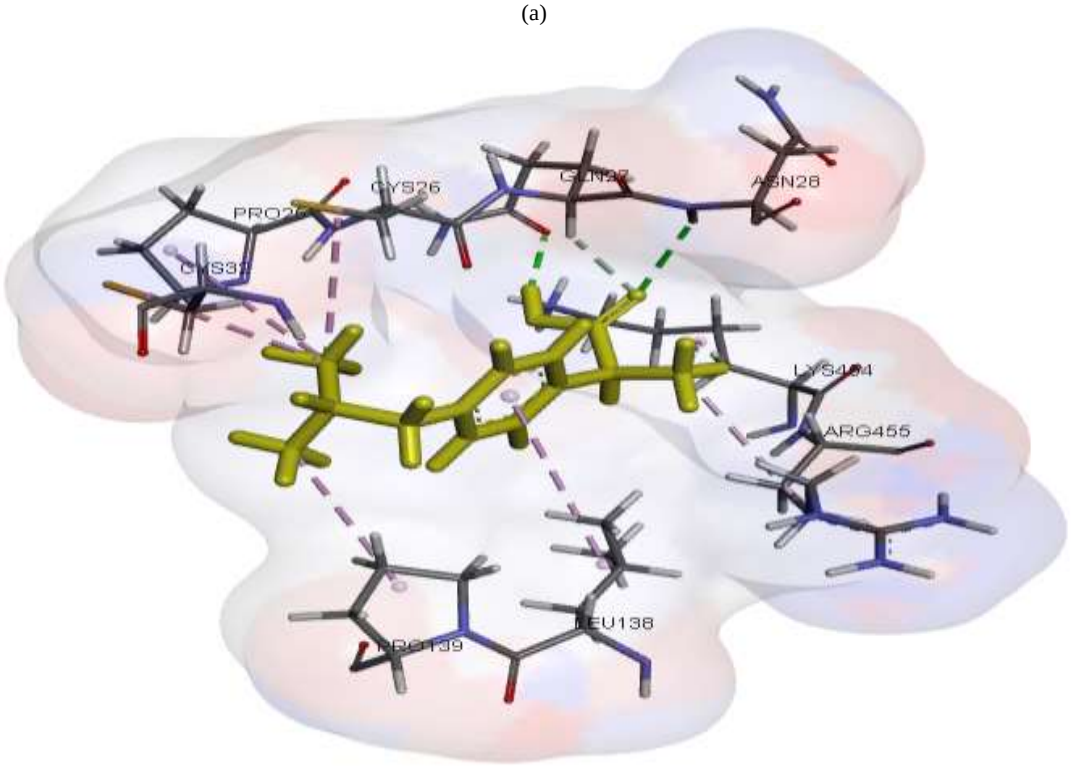

(b)

Figure 2 : Interaction of Ibuprofen with Cyclooxygenase-2 (COX-2). **(a)** 2D interaction showing the binding of Ibuprofen to residues within the COX-2 active site. **(b)** 3D visualization of Ibuprofen spatial orientation and binding pocket topology within the active site.

and CYS A:21, a halogen bond with CYS A:26, and hydrophobic contacts with TYR A:116, PRO A:139, LEU A:138, ARG A:455, and LYS A:454 (Figure 4). BS showed a binding energy of -7.1971 kcal/mol with COX-1 through conventional hydrogen bonds with ARG A:120 and GLU A:524, and hydrophobic contacts with LEU A:123, VAL A:119, ARG A:79, TYR A:64, and HIS A:43 (Figure 5). In COX-2, no hydrogen bonding was observed, but hydrophobic interactions were detected with CYS A:21, A:26, A:32, ARG A:29, A:455, LEU A:138, PRO A:139, and LYS A:454, resulting in a binding energy of -7.5424 kcal/mol (Figure 6). AXT displayed strong binding with COX-1 at -9.9239 kcal/mol, forming hydrophobic interactions with CYS A:36, A:47, HIS A:43, ILE A:46, LEU A:152,

ISSN 2616-0684 (Print)
ISSN 2616-0692 (Electronic)

PRO A:153, A:156, LYS A:468, and LYS A:473 (Figure 7). With COX-2, AXT demonstrated the highest binding energy of -10.4797 kcal/mol, involving extensive hydrophobic interactions with CYS A:21, A:32, ARG A:29, TYR A:122, PRO A:139, ALA A:142, and LYS A:454, and hydrogen bonding with SER A:457 (Figure 8). In the co-docked complex with COX-1, BS displayed a slightly improved binding energy (-7.6037

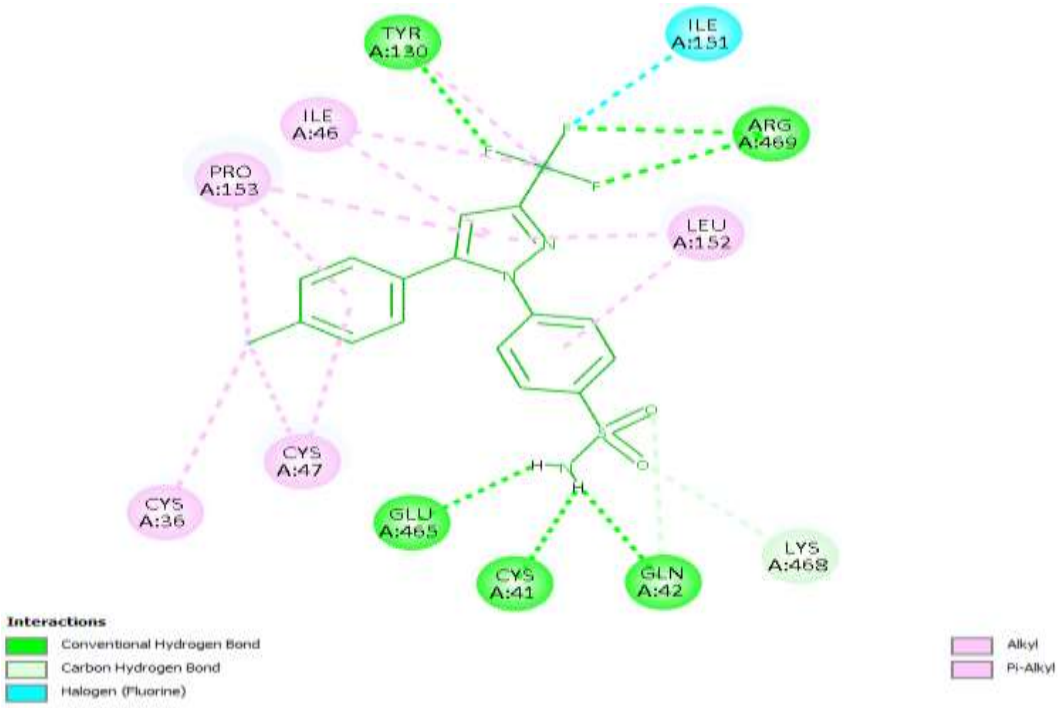

(a)

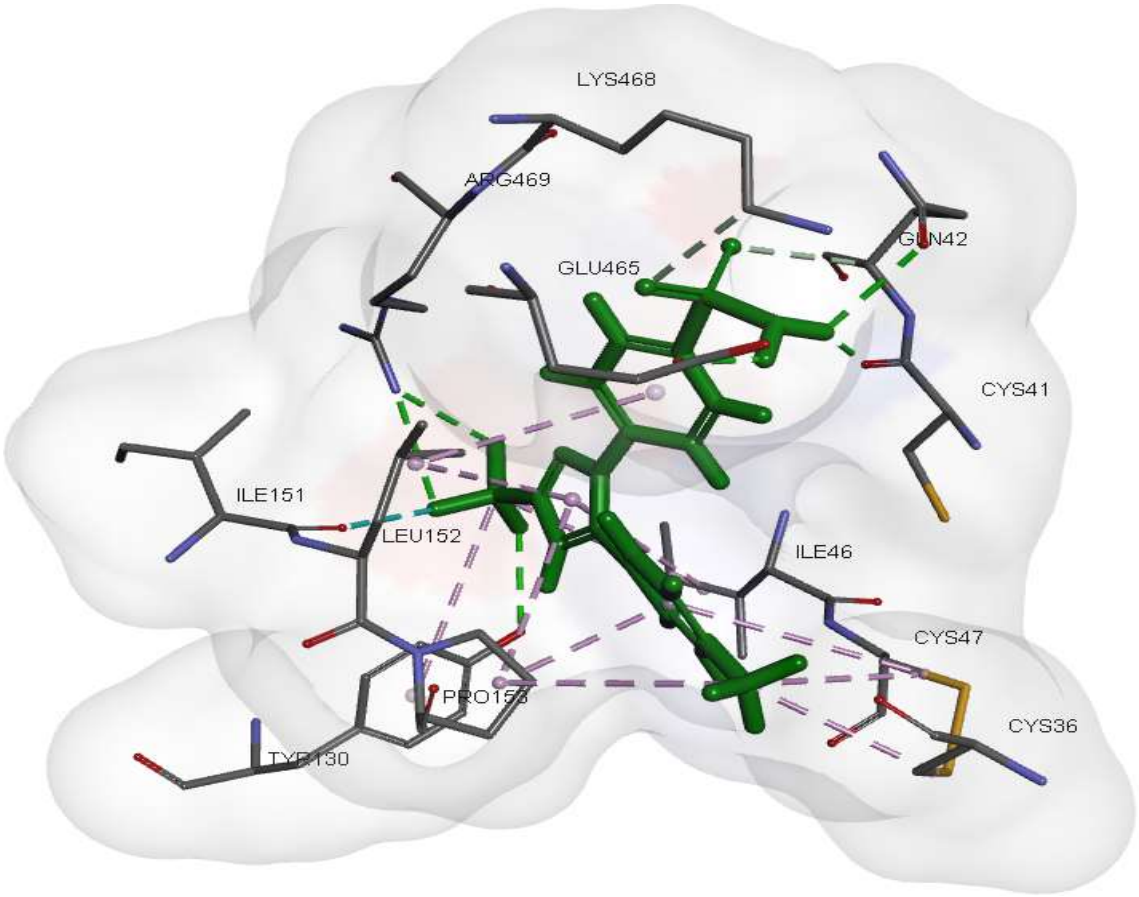

(b)

ISSN 2616-0684 (Print)
ISSN 2616-0692 (Electronic)

Figure 3 : Interaction of Celecoxib with Cyclooxygenase-1 (COX-1). **(a)** 2D interaction showing the binding of Celecoxib to residues within the COX-1 active site. **(b)** 3D visualization of Celecoxib spatial orientation and binding pocket topology within the active site.

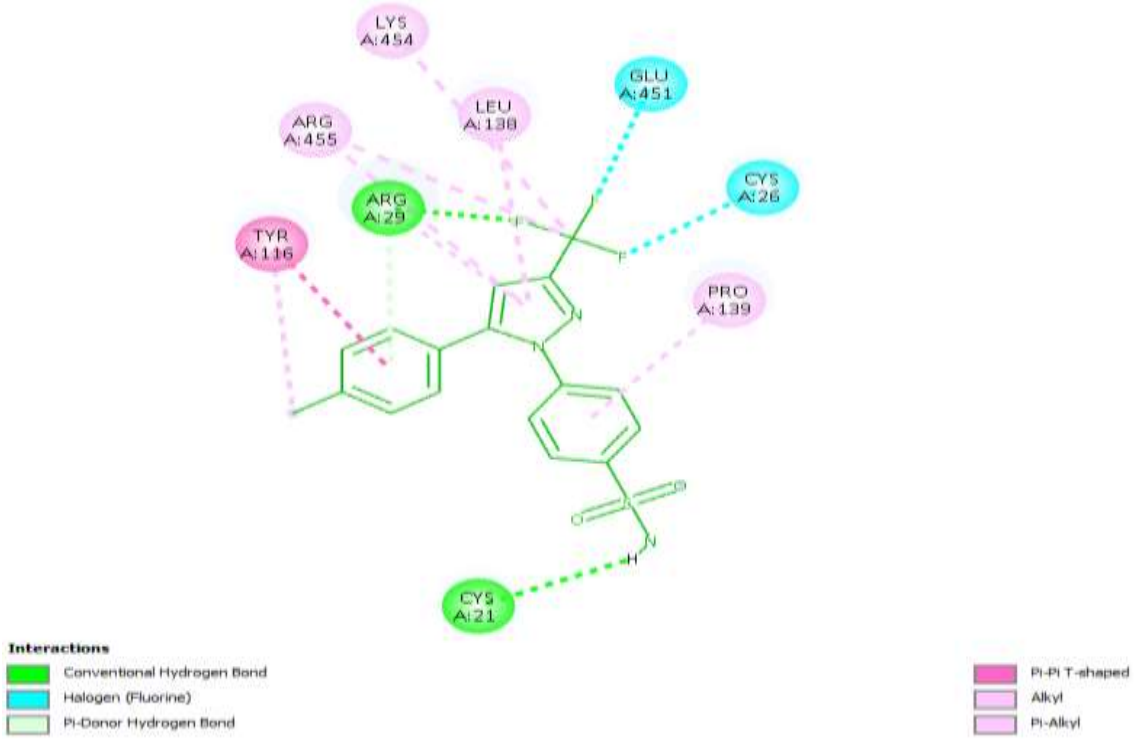

(a)

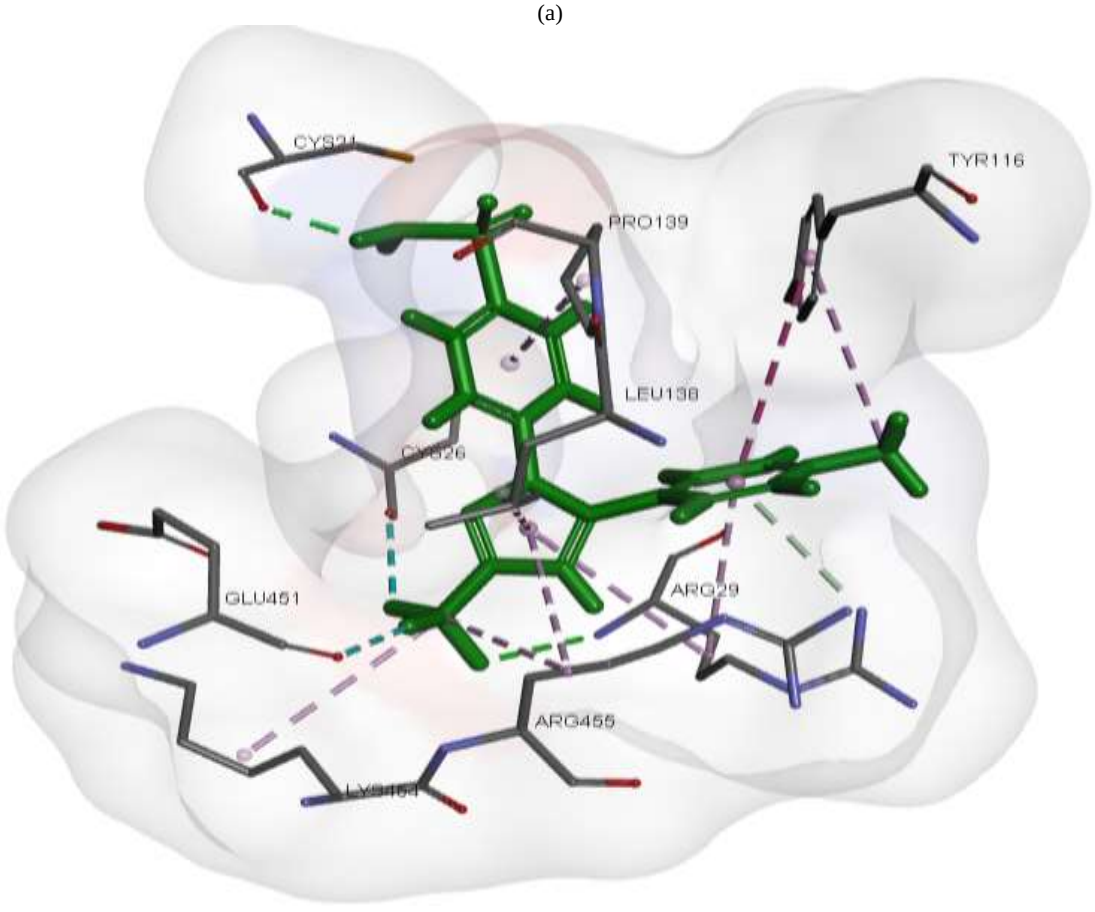

(b)

ISSN 2616-0684 (Print)
ISSN 2616-0692 (Electronic)

Figure 4 : Interaction of Celecoxib with Cyclooxygenase-2 (COX-2). **(a)** 2D interaction showing the binding of Celecoxib to residues within the COX-2 active site. **(b)** 3D visualization of Celecoxib spatial orientation and binding pocket topology within the active site.

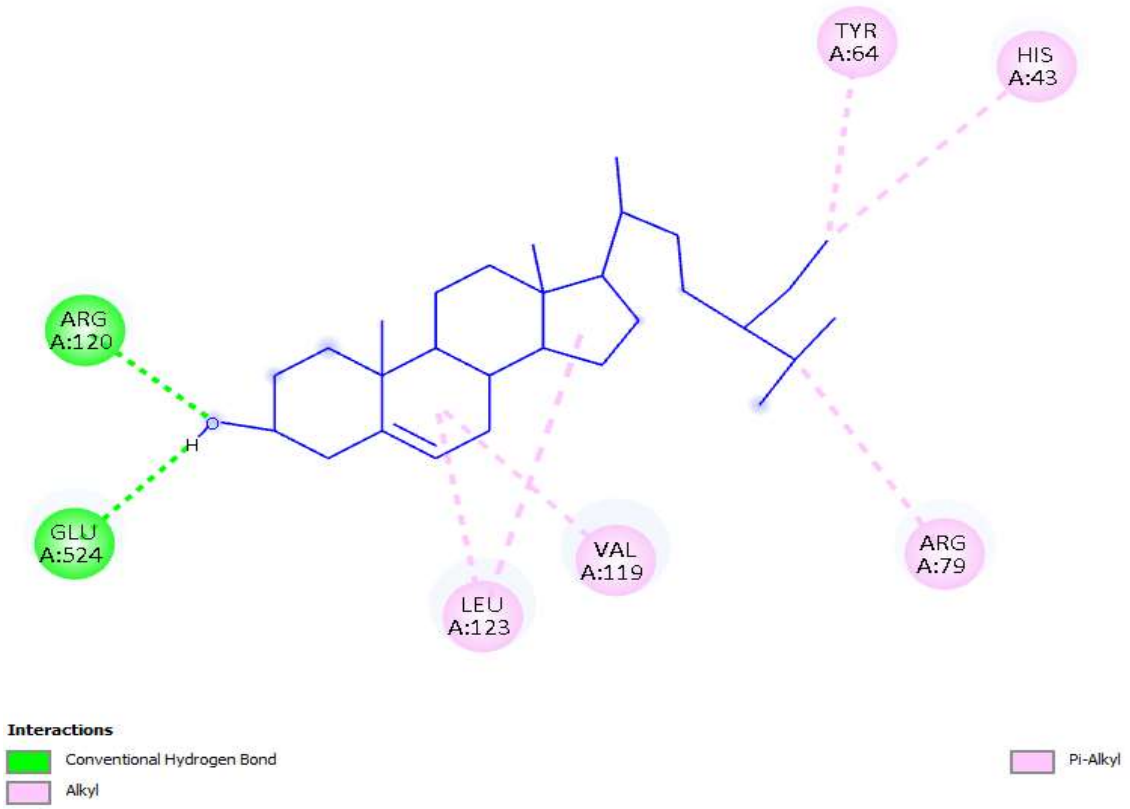

(a)

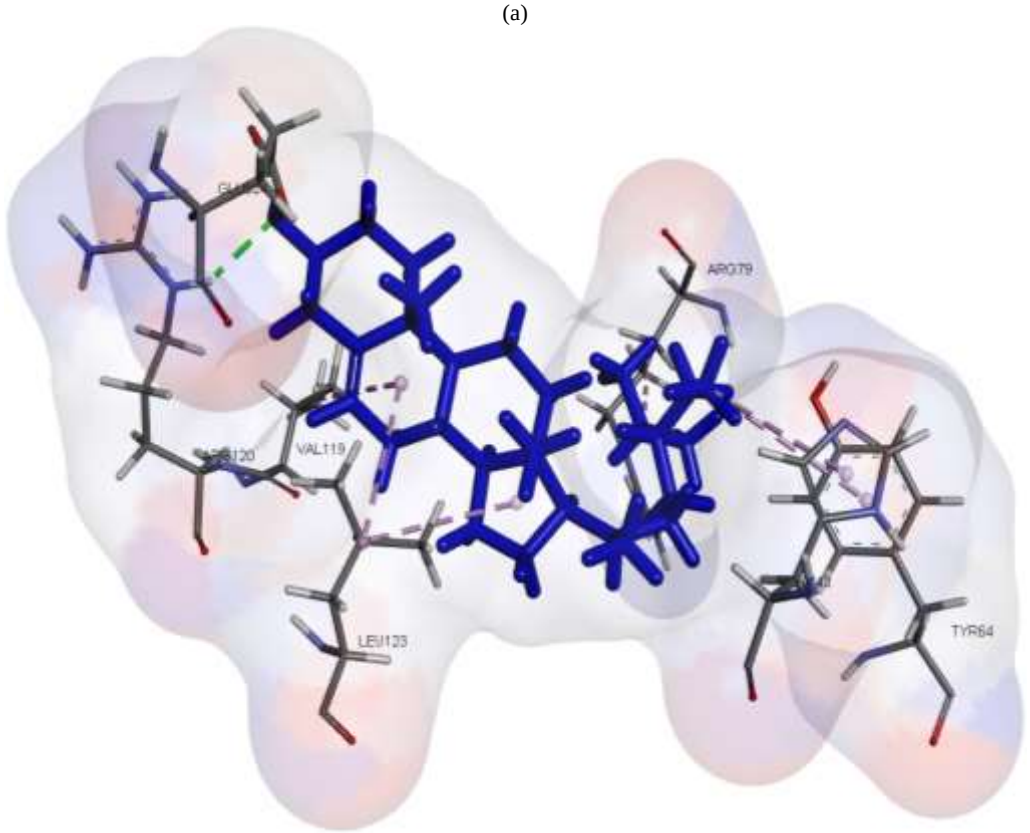

(b)

ISSN 2616-0684 (Print)
ISSN 2616-0692 (Electronic)

Figure 5 : Interaction of Beta-Sitosterol with Cyclooxygenase-1 (COX-1). **(a)** 2D interaction showing the binding of Beta-Sitosterol to residues within the COX-1 active site. **(b)** 3D visualization of Beta-Sitosterol spatial orientation and binding pocket topology within the active site

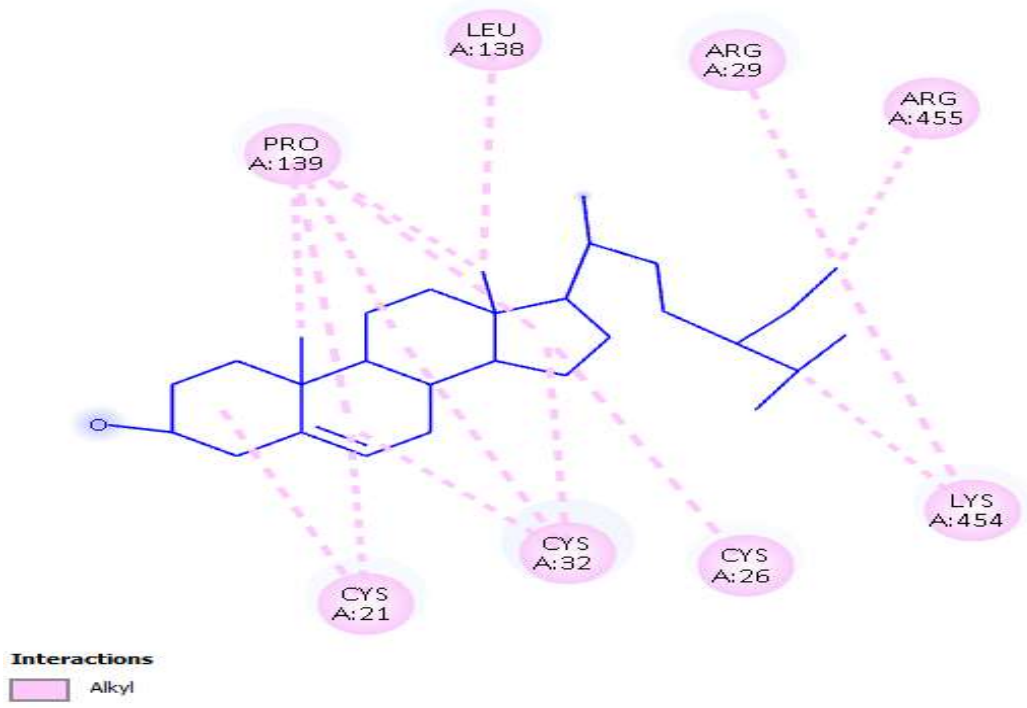

(a)

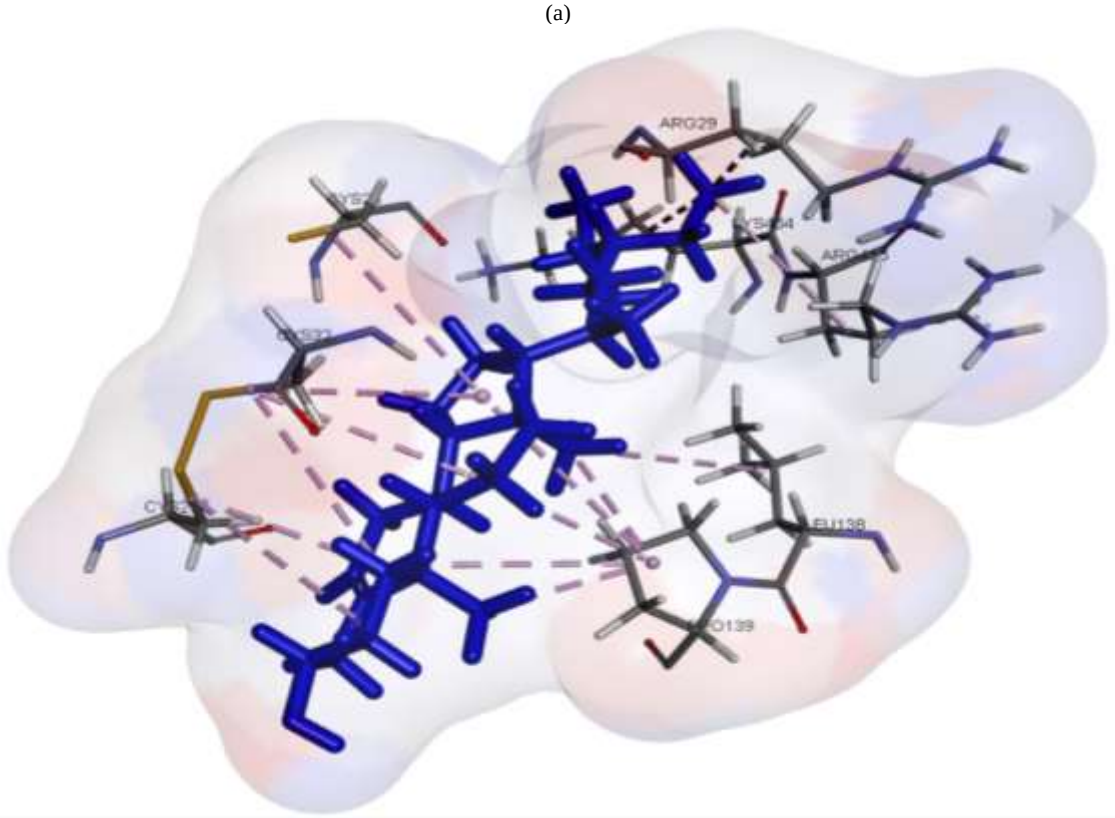

(b)

Figure 6 : Interaction of Beta-Sitosterol with Cyclooxygenase-2 (COX-2). **(a)** 2D interaction showing the binding of Beta-Sitosterol to residues within the COX-2 active site. **(b)** 3D visualization of Beta-Sitosterol spatial orientation and binding pocket topology within the active site.

ISSN 2616-0684 (Print)
ISSN 2616-0692 (Electronic)

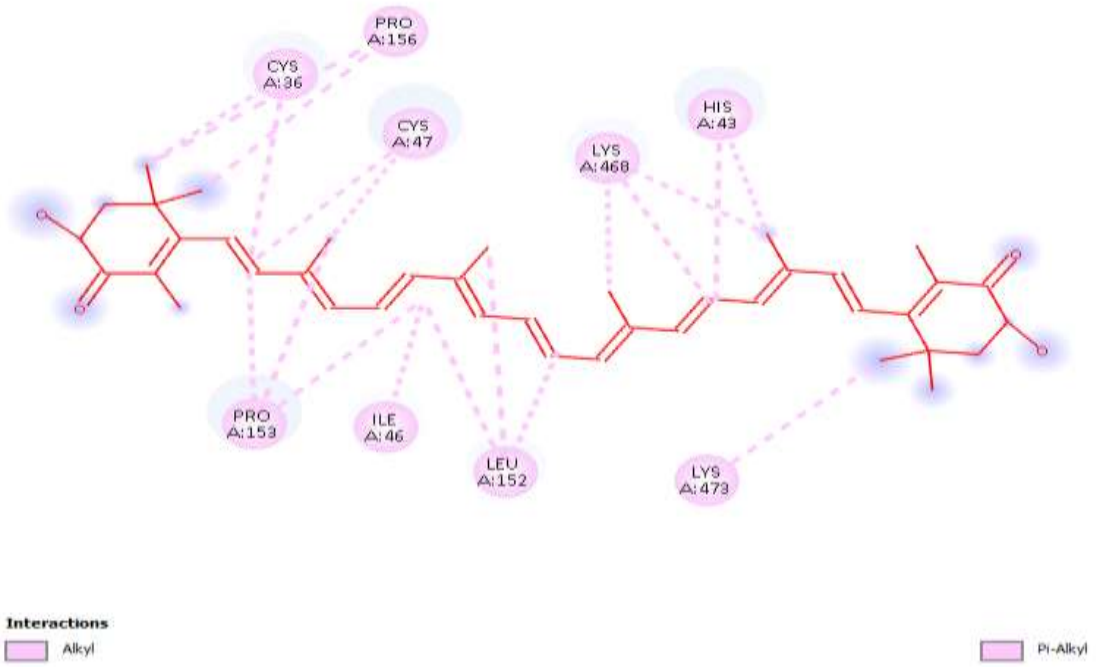

(a)

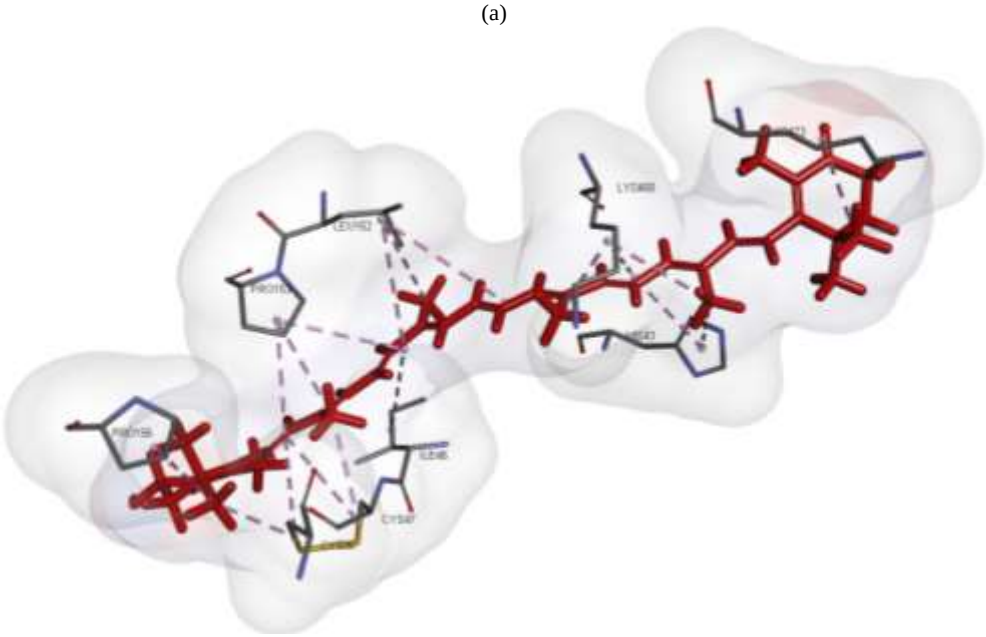

(b)

Figure 7: Interaction of Astaxanthin with Cyclooxygenase-1 (COX-1). **(a)** 2D interaction showing the binding of Astaxanthin to residues within the COX-1 active site. **(b)** 3D visualization of Astaxanthin spatial orientation and binding pocket topology within the active site.

kcal/mol), forming hydrogen bonds with HIS A:43, van der Waals interaction with LYS A:468, and hydrophobic interactions with CYS A:36, A:47, LEU A:152, PRO A:153, and A:156. AXT achieved enhanced binding (-10.0867 kcal/mol), forming pi-alkyl interactions with CYS A:36, A:47, HIS A:43, LEU A:152, PRO A:153, A:156, LYS A:468, and LYS A:473 (Figure 9). 2D interaction of complex Ligands binding within COX-1 active site also shown in Figure 10.

BS in complex form had enhanced binding energy of -9.2033 kcal/mol, forming a carbon-hydrogen bond with ASN A:28 and hydrophobic contacts with CYS A:21, A:32, ARG A:29, LEU A:138, PRO A:139, ALA A:142, LYS A:454, and ARG A:455. AXT showed the strongest overall affinity (-10.7948 kcal/mol), forming hydrogen bonds with SER A:457 and LYS A:68, and extensive hydrophobic interactions with CYS A:21, A:32, ARG A:29, PRO A:139, ALA A:142, LYS:454, and PRO A:460 (Figure 11). 2D interaction of complex Ligands binding within COX-1 active site also shown in Figure 12.

As shown in Table 3, IB and BS did not share any common interacting residues with COX-1. However, IB and AXT shared CYS A:36, HIS A:43, CYS A:47, LEU A:152, PRO A:153, and LYS A:468. No overlapping residue was observed between CX and BS, whereas CX and AXT shared CYS A:36, ILE A:152, and PRO A:153. In the

ISSN 2616-0684 (Print)
ISSN 2616-0692 (Electronic)

combination form, IB and BS showed common residues of CYS A:36, CYS A:47, LEU A:152, and PRO A:153, while IB and AXT showed CYS A:36 and CYS A:47. CX and BS shared CYS A:36, CYS A:47,

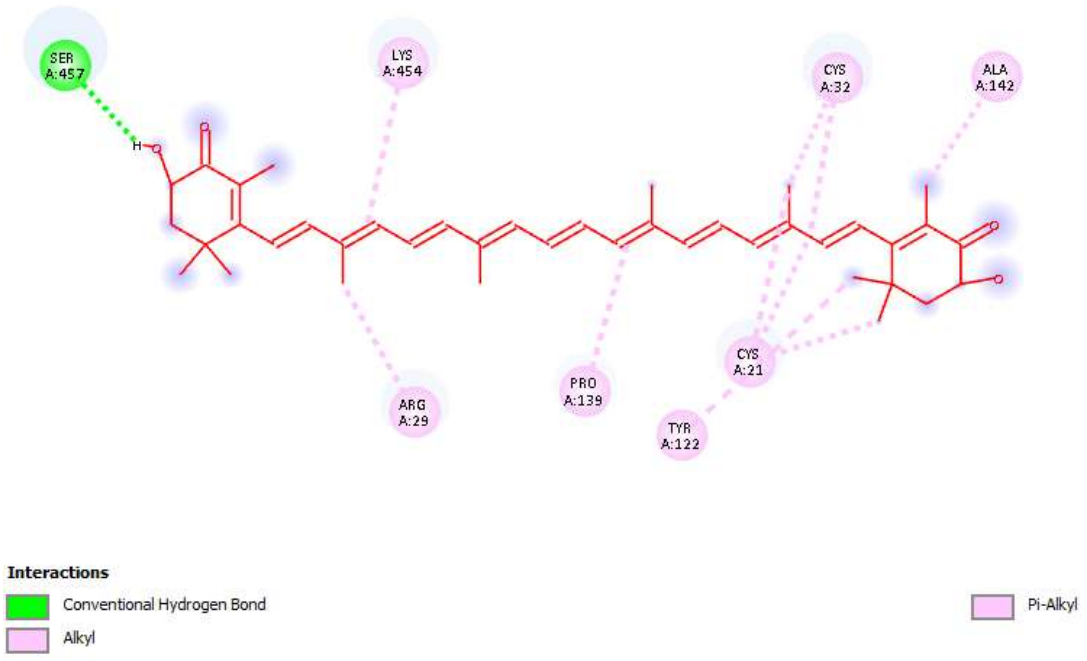

(a)

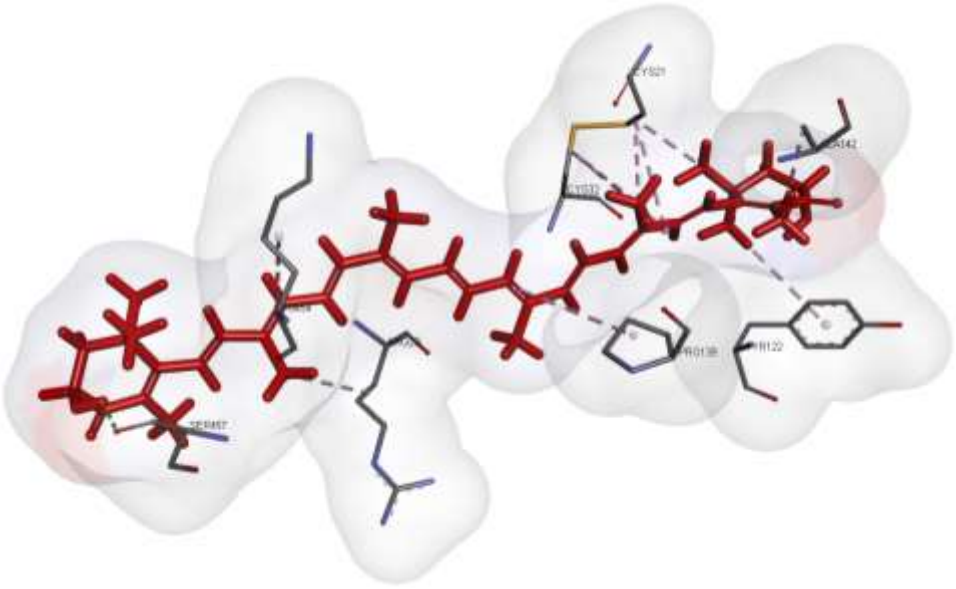

(b)

Figure 8 : Interaction of Astaxanthin with Cyclooxygenase-2 (COX-2). **(a)** 2D interaction showing the binding of Astaxanthin to residues within the COX-2 active site. **(b)** 3D visualization of Astaxanthin spatial orientation and binding pocket topology within the active site.

LEU A:152, and PRO A:153, while CX and AXT interactions included CYS A:36, LEU A:152, and PRO A:156.

For COX-2, IB and BS shared CYS A:26, CYS A:32, LEU A:138, PRO A:139, LYS A:454, and ARG A:455. IB and AXT overlapped with CYS A:32, PRO A:139, and LYS A:454. CX and BS shared CYS A:21, ARG A:29, PRO A:139, LYS A:454, and ARG A:455, whereas CX and AXT shared CYS A:21, ARG A:29, and LYS A:454. In the combination form, IB and BS shared ASN A:28, CYS A:32, LEU A:138, PRO A:139, and LYS A:454. CX and BS shared CYS A:21, ARG A:29, PRO A:139, LYS A:454, and ARG A:455, whereas CX and AXT shared CYS A:21, ARG A:29, and LYS A:454. The binding

ISSN 2616-0684 (Print)
ISSN 2616-0692 (Electronic)

energies of each ligand against COX isoforms are summarized as follows:

COX-1: AXT (combination, -10.0867) > AXT (single, -9.9239) > BS (combination, -7.6037) > CX (-7.4058) > BS (single, -7.1971) > IB (-6.3164

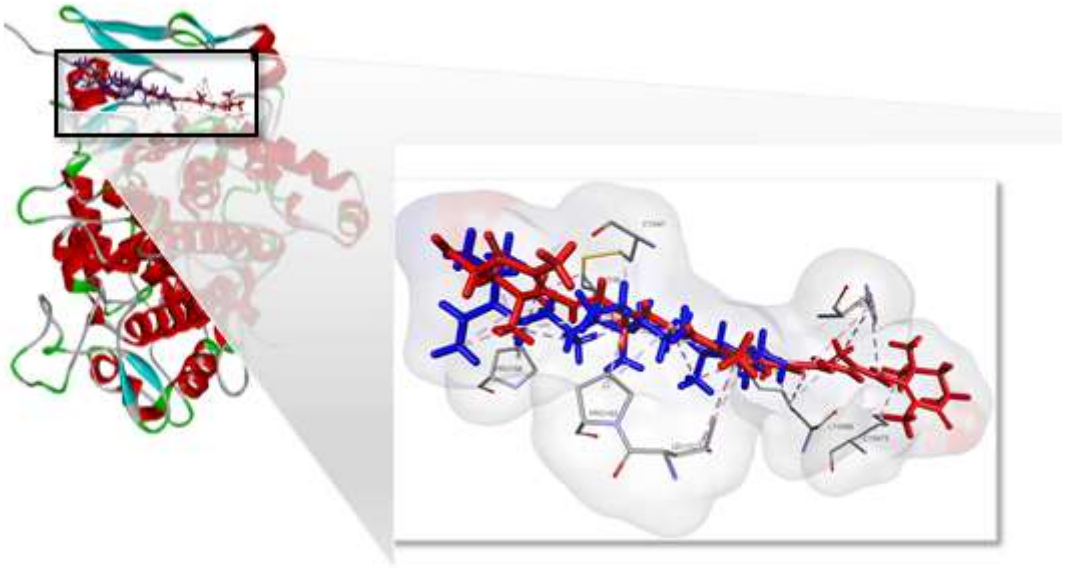

Figure 9 : Binding of Complex into COX-1 active site binding pocket

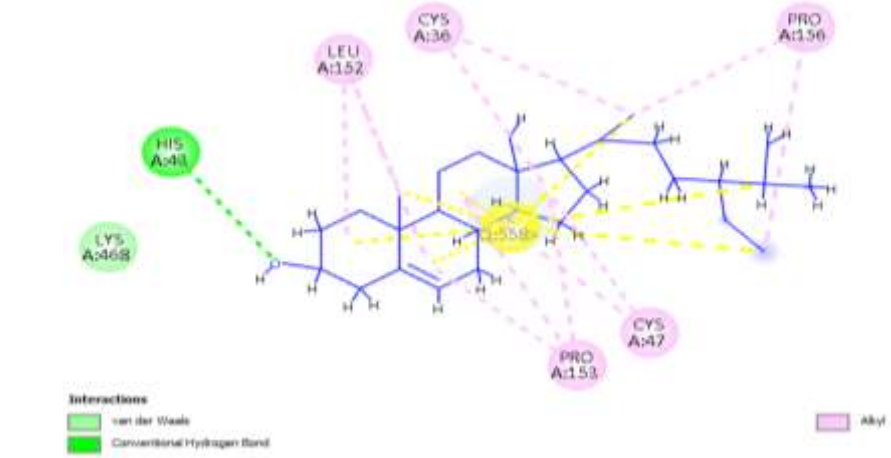

(a)

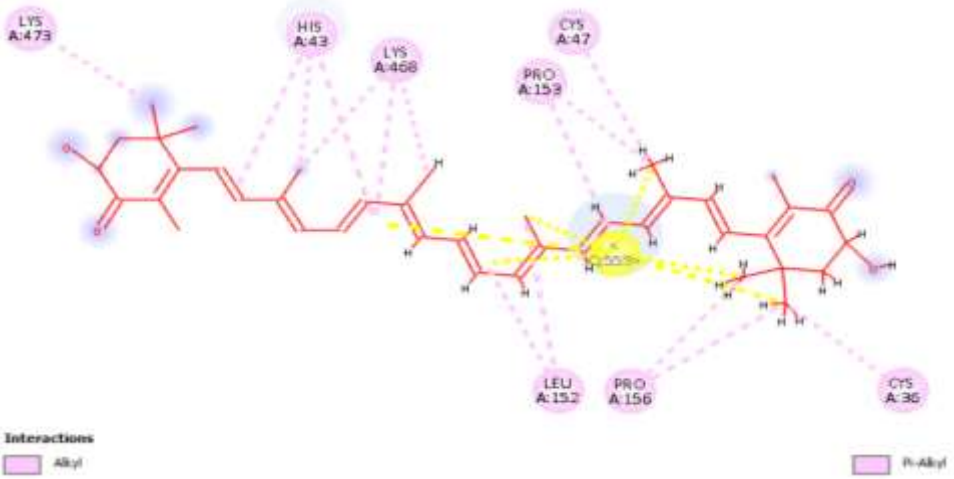

(b)

ISSN 2616-0684 (Print)
ISSN 2616-0692 (Electronic)

Figure 10 : 2D interaction of complex Ligands binding within COX-1 active site. **(a)** Beta-Sitosterol, **(b)** Astaxanthin.

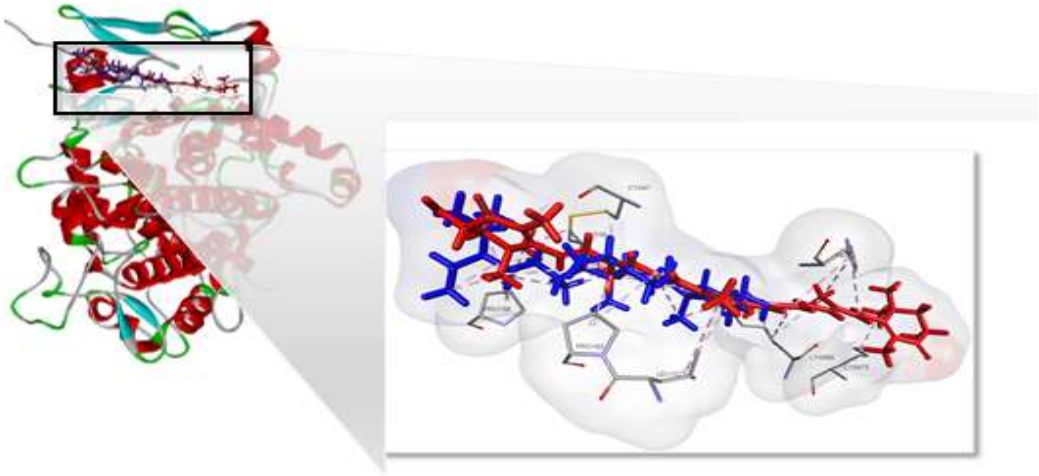

Figure 11 : Binding of Complex into COX-2 active site binding pocket

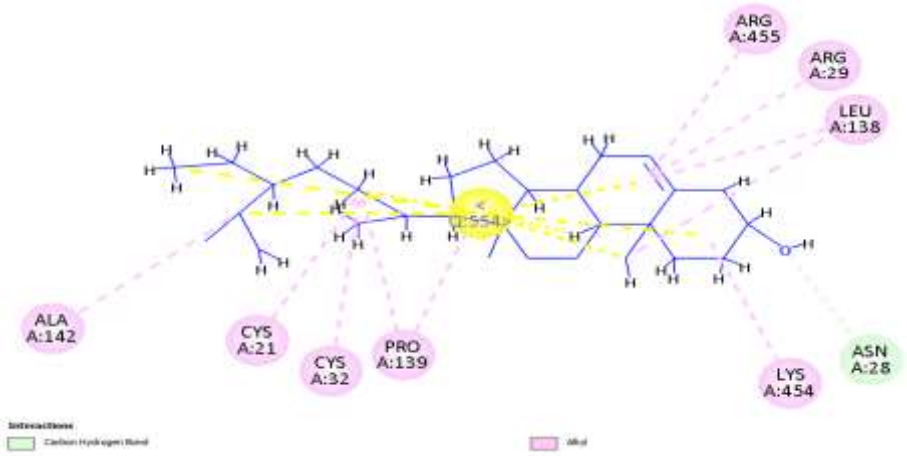

(a)

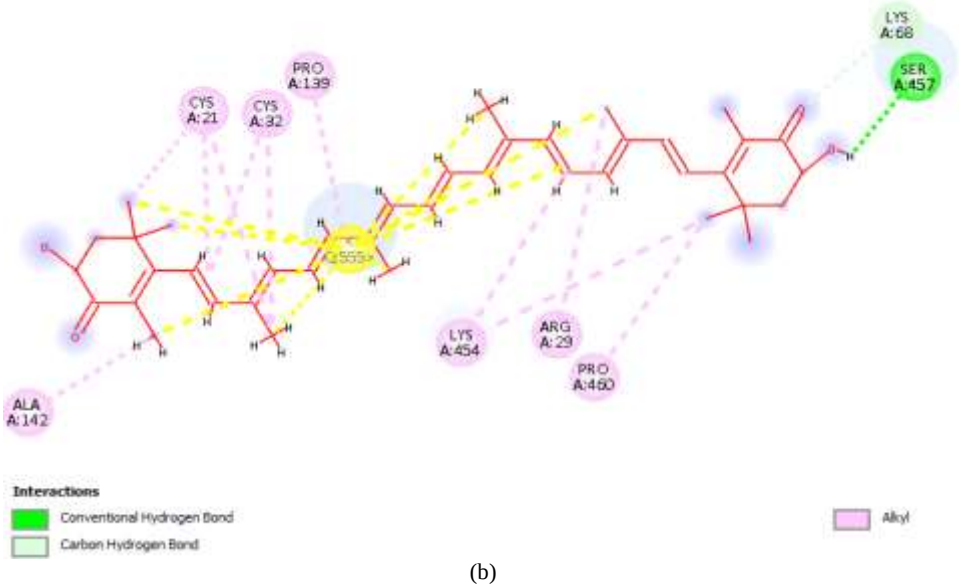

(b)

Figure 12 : 2D interaction of complex Ligands binding within COX-2 active site. **(a)** Beta-Sitosterol, **(b)** Astaxanthin.

ISSN 2616-0684 (Print)
ISSN 2616-0692 (Electronic)

Table 1 : Molecular docking interactions of Ligands into COX-1

Name of Ligand	Binding Energy (kcal/mol)	RMSD Value	Hydrogen Bonding		Hydrophobic Interactions	
			Conventional	Carbon-Hydrogen	Alkyl and Pi-Alkyl	Others
Ibuprofen	-6.3164	1.6322	HIS A:43 LYS A:468		CYS A:36 PRO A:40 CYS A:41 CYS A:47 LEU A:152 PRO A:153 ARG A:469	
Celecoxib	-7.4058	1.2051	CYS A:41 GLN A:42 TYR A:130 ARG A:469 GLU A:465	LYS A: 468	CYS A:36 ILE A:46 CYS A:47 LEU A:152 PRO A:153	ILE A: 151 (Halogen – Fluorine)
Beta-Sitosterol (Single)	-7.1971	1.7905	ARG A:120 GLU A:524		HIS A:43 TYR A:64 ARG A:79 VAL A:119 LEU A:123	
Astaxanthin (Single)	-9.9329	1.0690			CYS A:36 HIS A:43 ILE A:46 CYS A:47 LEU A:152 PRO A:153 PRO A:156 LYS A:468 LYS A:473	
Beta-Sitosterol (Complex)	-7.6037	1.6251	HIS A:43		CYS A:36 CYS A:47 LEU A:152 PRO A:153 PRO A:156	LYS A:468 (Van der Waals)
Astaxanthin (Complex)	-10.0867	1.8291			CYS A:36 HIS A:43 ILE A:46 CYS A:47 LEU A:152 PRO A:156 LYS A:468 LYS A:473	

ISSN 2616-0684 (Print)
ISSN 2616-0692 (Electronic)

COX-2: AXT (combination, -10.7948) > AXT (single, -10.4797) > BS (combination, -9.2033) > CX (-7.5955) > BS (single, -7.5424) > IB (-6.2170)
The BS binding energy improved from -7.5424 kcal/mol to -9.2033 kcal/mol for COX-2, particularly in complex form, suggesting a synergistic effect when combined with AXT.

This study was performed to investigate the potential synergistic effect of BS-AXT combination on COX enzymes using molecular docking techniques. This study aimed to compare the binding affinity and interaction profiles of BS-AXT in combination with individual compounds and standard COX inhibitors including ibuprofen (IB) and celecoxib (CX). The structural features of BS and AXT enable key

Table 2 : Molecular docking interactions of Ligands into COX-2

Name of Ligand	Binding Energy (kcal/mol)	RMSD Value	Hydrogen Bonding		Hydrophobic Interactions	
			Conventional	Carbon-Hydrogen	Alkyl and Pi-Alkyl	Others
Ibuprofen	-6.2170	1.1298	GLN A:27		PRO A:25	
			ASN A:28		CYS A:26	
					CYS A:32	
					LEU A:138	
					PRO A:139	
					LYS A:454	
					ARG A:455	
Celecoxib	-7.5955	1.6054	CYS A: 21		LEU A:138	CYS A:26
			ARG A: 29		PRO A:139	(Halogen-Fluorine)
					LYS A:454	TYR A:116
					ARG A:455	(Pi-Pi T-shaped)
						GLU A:451
						(Halogen-Fluorine)
Beta-Sitosterol	-7.5424	0.6867			CYS A:21	
(Single)					CYS A:26	
					ARG A:29	
					CYS A:32	
					LEU A:138	
					PRO A:139	
					LYS A:454	
					ARG A:455	
Astaxanthin	-10.4797	0.9583	SER A:457		CYS A:21	
(Single)					ARG A:29	
					CYS A:32	
					TYR A:122	
					PRO A:139	
					ALA A:142	
					LYS A:454	
Beta-Sitosterol	-9.2033	1.1713		ASN A:28	CYS A:21	
(Complex)					ARG A:29	
					CYS A:32	
					LEU A:138	
					PRO A:139	
					ALA A:142	
					LYS A:454	
					ARG A:455	

ISSN 2616-0684 (Print)
ISSN 2616-0692 (Electronic)

Astaxanthin (Complex)	-10.7948	1.2850	SER A:457	LYS A:68	CYS A:21 ARG A:29 CYS A:32 PRO A:139 ALA A:142 LYS A:454 PRO A:460

Table 3 : Common amino acid residues interactions among ligands

Protein	Ligand Pairs	Common Interactions
COX-1	Ibuprofen and Beta-Sitosterol	–
	Ibuprofen and Astaxanthin	CYS A:36, HIS A:43, CYS A:47, LEU A:152, PRO A:153, LYS A:468
	Celecoxib and Beta-Sitosterol	–
	Celecoxib and Astaxanthin	CYS A:36, ILE A:46, CYS A:47, LEU A:152, PRO A:153
	Ibuprofen and Beta Sitosterol Complex	CYS A:36, CYS A:47, LEU A:152, PRO A:153
	Ibuprofen and Astaxanthin Complex	CYS A:36, CYS A:47, LEU A:152
	Celecoxib and Beta Sitosterol Complex	CYS A:36, CYS A:47, LEU A:152, PRO A:153
	Celecoxib and Astaxanthin Complex	CYS A:36, CYS A:47, LEU A:152, CYS A:468
COX-2	Ibuprofen and Beta-Sitosterol	CYS A:26, CYS A:32, LEU A:138, PRO A:139, LYS A:454, ARG A:455
	Ibuprofen and Astaxanthin	CYS A:32, PRO A:139, LYS A:454
	Celecoxib and Beta-Sitosterol	CYS A:21, ARG A:29, LEU A:138, PRO A:139, LYS:454, ARG A:455
	Celecoxib and Astaxanthin	CYS A: 21, ARG A:29, PRO A:139, LYS A:454
	Ibuprofen and Beta Sitosterol Complex	ASN A:28, CYS A:32, LEU A:138, PRO A:139, LYS A:454, ARG A:455
	Ibuprofen and Astaxanthin Complex	CYS A:32, PRO A:139, LYS A:454
	Celecoxib and Beta Sitosterol Complex	CYS A:21, ARG A:29, LEU A:138, PRO A:139, LYS A:454, ARG A:455
	Celecoxib and Astaxanthin Complex	CYS A:21, ARG A:29, CYS A:32, PRO A:139, LYS A:454

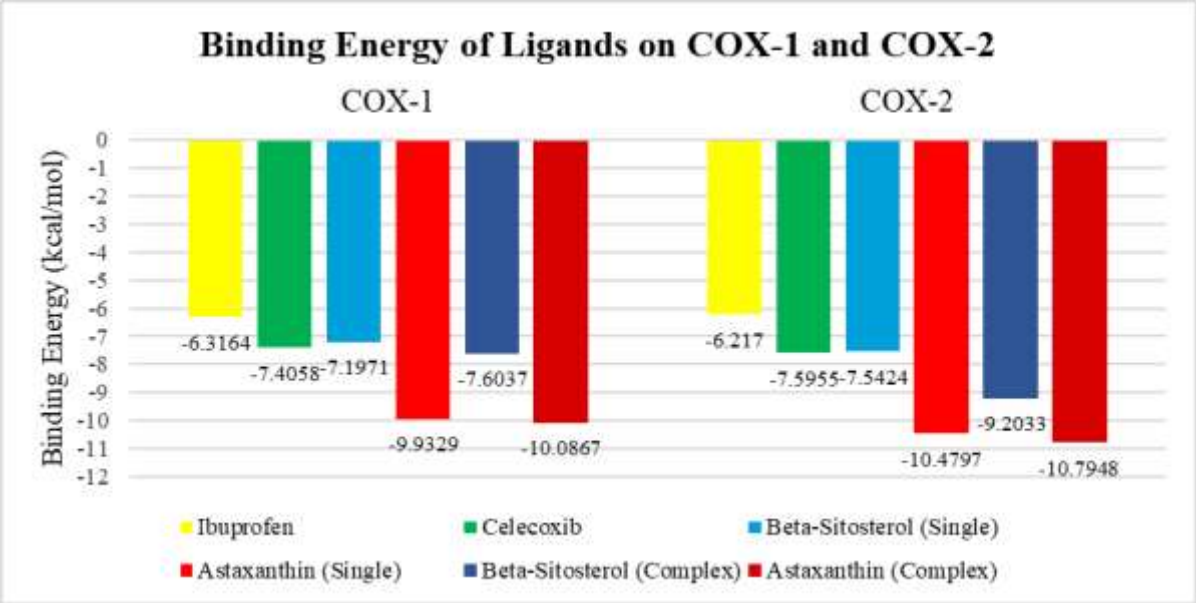

Figure 13 : Binding Energy of Ligands on COX-1 and COX-2 Bar Chart

interactions with both the COX isoforms. BS has a hydrophobic steroid backbone, while AXT has a long-conjugated polyene chain, allowing the formation of hydrogen bonds, pi-alkyl stacking, and hydrophobic interactions, which help stabilize the ligand-protein complex, contributing to COX inhibition.[16,17] The docking results suggested a possible selective COX-2 inhibition over COX-1, which is a desirable trait in anti-inflammatory drug design.

COX-1 and COX-2 have almost identical active sites, but differ in key residues, such as Ile523 in COX-1 and Val523 in COX-2, allowing the COX-2 isoform to bind with bulkier ligands. Residues such as Arg120, Tyr355, and Glu524 form the active site entrance, whereas Arg513 and Val434 in COX-2 improve ligand fit through polar and spatial interactions to determine how inhibitors selectively bind to COX-2.[18,19] Pharmacophore models highlighting the importance of hydroxyl, carboxyl, and hydrophobic groups for effective interactions with key residues, such as Arg120, Tyr 355, and Val523. Asiatic acid showed good binding energy and mimicked COX-2 inhibitors, such as CX, owing to its carboxyl group.[20]

BS is a plant sterol that is structurally similar to cholesterol, comprising a steroid backbone as a core structure and a long hydrophobic chain at C17 with one polar hydroxyl group attached at C3.[16] This hydrophobic structure allows BS to enter the lipophilic COX pocket, interacting mainly through van der Waals and hydrophobic interactions with nonpolar residues, such as alanine, valine, and leucine, and hydrogen bonding is limited because of the less polar group.[21,22,23] The binding energies of BS to COX-1 and COX-1 were -7.1971 kcal/mol and -7.5424 kcal/mol, respectively. In the previous studies, BS interaction with COX preferentially bound to COX-2 over COX-1, as evidenced by the stronger binding energy of COX-2, as per our study. The binding energies produced by BS on COX varies across studies, ranging from -3.1 kcal/mol to -5.5 kcal/mol on COX-1,[24,25,26] and -6.54 kcal/mol to -12.38 kcal/mol,[27,28,29,30] depending on the protein conformation and docking tools with most of them had the average of -7 kcal/mol on COX-2 especially, which was comparable with our study. In all these cases, BS mainly interacted with hydrophobic residues, such as valine, leucine, tyrosine, and phenylalanine.

Binding interactions with COX isoforms were mainly hydrophobic at residues Cys21, Cys32, Leu138, Arg120, and Tyr64. As shown in Table 3, BS in single docking did not show direct overlapping of the interaction residues with either IB or CX. However, in the combination form with CX or IB, common residues such as CYS A:36, LEU A:152, and PRO A:152 were observed, suggesting that BS binding affinity was enhanced when in combination. Meanwhile, on COX-2, BS demonstrated stronger overlap with standard inhibitors interacting residues, such as CYS A:21, ARG A:29, PRO A:139, LYS A:454, and ARG A:454, which were identified in both single and combination forms. These residues are essential for COX-2 binding and catalytic activity, indicating that BS may closely mimic the orientation and interactions of the COX-2 selective inhibitor CX. Studies have consistently reported that BS binds to common COX-2 residues such as Tyr255, Leu352, Val349, Ala527, and Met522. [28,29,30] Important residues, such as Tyr385 and Arg120, play important roles in substrate binding and peroxidase function, and appear repeatedly in COX-1 and COX-2 docking studies. This indicates that these residues may act as conserved binding hotspots for BS.[27,31,32]

AXT is a carotenoid with a long, conjugated polyene chain that makes it hydrophobic, and shares a similar structure with other carotenoids, such as beta-carotene and lycopene, which helps it fit into the hydrophobic pocket of the COX active site.[17,33] Because of this similarity, it is often compared with other carotenoids.[34] Although AXT shares this similarity, its additional polar groups (hydroxyl and keto) at the ends of the chain differ from those of other the carotenoids, making it more amphipathic.[35] The binding energy of AXT showed favorable binding to COX-2 compared to COX-1, as demonstrated by the stronger binding energies of -10.4797 kcal/mol for COX-2 and -9.9239 kcal/mol for COX-1. Prior research demonstrated that the AXT binding energy on COX-1 was -8.2 kcal/mol,[11] while on COX-2, it ranged from -7.2 to -8.722 kcal/mol,[36,37,38] which were considered strong binding, although lower than those obtained in our study.

As shown in Table 3, AXT showed more promising individual overlap with standard COX-1 interactions than BS. In COX-1, AXT alone shared residues such as CYS A:36, LEU A:152, and PRO A:153 with both IB and CX. The presence of these overlapping residues suggests that AXT binds to a similar region of the active site as standard NSAIDs, supporting its potential to inhibit COX-1 activity on its own. On COX-2, AXT exhibited favorable alignment with standard inhibitors. Residues such as PRO A:139 and LYS A:454 were shared with IB and CX. The conservation of these interactions indicates that AXT, similar to BS, may engage in critical COX-2 residues that are essential for effective inhibition. Previous docking studies showed that AXT bound COX-2 preferentially compared to COX-1 through hydrophobic interactions (alkyl and pi-alkyl) with residues such as Lys211, His214, and Val291, as well as hydrogen bonding with His386 and Asn382.[11,37,38]

Through the combination docking of BS and AXT, this study demonstrated an enhancement in the binding energy of BS to COX-2, which improved from -7.5424 kcal/mol in single docking to -9.2033 kcal/mol in combination docking with AXT. This enhanced binding energy was also higher than that of standard COX inhibitors, as presented in Table 2 and Figure 13. This enhancement indicated a synergistic effect of the combination, proving that AXT might help BS to interact with the COX-2 pocket through an *in silico* approach. Although no previous study has directly explored the combination of BS and AXT on COX, existing evidence suggests that combining a lipophilic compound, such as BS, with the antioxidant AXT may enhance its binding and biological effects. Both compounds showed synergistic effects when combined with other agents. BS improved anticancer effects in combination with hydrastinine and stigmasterol.[39,40] Meanwhile, AXT enhanced the anti-inflammatory action of celecoxib, and boosted antioxidant and anti-inflammatory response in the mixed compounds with vitamin C, collagen peptides, and resveratrol.[41,42] This finding supports the potential of BS and AXT to work together more effectively than individually, possibly leading to stronger COX inhibition through complementary binding interactions.

Conclusion

The combination of BS and AXT produced stronger and more stable binding to COX-2 than either compound alone, as evidenced by the improved BS binding energy from -7.5424 kcal/mol (alone) to -9.2033 kcal/mol (combination) for COX-2. It demonstrated improvement in binding affinity and interaction diversity, particularly through enhanced hydrophobic contacts from BS and AXT, and additional hydrogen bonds contributed by AXT. These complementary interactions suggest a possible synergistic effect that stabilizes the ligand-protein complex, especially within the COX-2 pocket. This binding pattern resembled that of known COX-2 inhibitors, indicating potential for reduced side effects. These findings support the concept that the combination of phytosterol and xanthophyll carotenoids can naturally enhance COX-2 inhibition. Further *in vitro* and *in vivo* studies are necessary for the verification of these promising results.

Conflict of interest

The author`s declare no conflict of interest.

Authors' Declaration

The authors hereby declare that the work presented in this article is original and that any liability for claims related to the content of this article will be borne by them.

Acknowledgements

The authors would like to express their gratitude to the Faculty of Pharmacy for providing research facilities.

References

1. Oyesola OO, Tait ED. Prostaglandin regulation of type 2 inflammation: From basic biology to therapeutic interventions. Eur J Immunol. 2021; 51(10):2399–2416.
2. Faki Y, Er A. Different chemical structures and physiological/pathological roles of cyclooxygenases. Rambam Maimonides Med J. 2021; 12(1):1–13.

3. Araújo PHF, Ramos RS, da Cruz JN, Silva SG, Ferreira EFB, de Lima LR, Macêdo WJC, Espejo-Román JM, Campos JM, Santos CBR. Identification of potential COX-2 inhibitors for the treatment of inflammatory diseases using molecular modeling approaches. Molecules. 2020; 25(18):1–32.
4. Chan PC, Liao MT, Hsieh PS. The dualistic effect of COX-2-mediated signaling in obesity and insulin resistance. Int J Mol Sci. 2019; 20(13):1–13.
5. Er-Rajy M, El-Fadili M, Mujwar S, Imtara H, Al kamaly O, Zuhair Alshawwa S, Nasr FA, Zarougui S, Elhallaoui M. Design of novel anti-cancer agents targeting COX-2 inhibitors based on computational studies. Arab J Chem. 2023; 16(10):1–18.
6. Darkazally AZ, Alnour A, Homsi S. Troxerutin effect on gastric ulcers induced by ketorolac in rats: Relation with oxidative stress. Heliyon. 2024; 10(19):1–11.
7. Zhang K, Yuan G, Werdich AA, Zhao Y. Ibuprofen and diclofenac impair the cardiovascular development of zebrafish (*Danio rerio*) at low concentrations. Environ Pollut. 2020; 258(2020):1–37.
8. Zheng Y, Zhao J, Chang S, Zhuang Z, Waimei S, Li X, Chen Z, Jing B, Zhang D, Zhao G. β-Sitosterol Alleviates Neuropathic Pain by Affect Microglia Polarization through Inhibiting TLR4/NF-κB Signaling Pathway. J Neuroimmune Pharmacol. 2023; 18(4):690–703.
9. Tallapalli PS, Reddy YD, Yaraguppi DA, Matangi SP, Challa RR, Vallamkonda B, Ahmad SF, Al-Mazroua HA, Rudrapal M, Dintakurthi SNBKP, Pasala PK. In Silico and In Vivo Studies of β-Sitosterol Nanoparticles as a Potential Therapy for Isoprenaline-Induced Cognitive Impairment in Myocardial Infarction, Targeting Myeloperoxidase. Pharmaceuticals. 2024; 17(8):1–22.
10. Peng YJ, Lu JW, Liu FC, Lee CH, Lee HS, Ho YJ, Hsieh TH, Wu CC, Wang CC. Astaxanthin attenuates joint inflammation induced by monosodium urate crystals. FASEB J. 2020; 34(8):11215–11226.
11. Alam A, Tamkeen N, Imam N, Farooqui A, Ahmed MM, Tazyeen S, Ali S, Malik MZ, Ishrat R. Pharmacokinetic and molecular docking studies of plant-derived natural compounds to exploring potential anti-Alzheimer activity. In: In Silico Approach for Sustainable Agriculture. Springer Singapore; 2018; 3(2018):217–238.
12. Ijoma IK, Okafor CE, Ajiwe VIE. Computational Studies of 5-methoxypsolaren as Potential Deoxyhemoglobin S Polymerization Inhibitor. Trop J Nat Prod Res. 2024; 8(10):8835–8841.
13. Zubair MS, Yuyun Y, Musnina WS, Najib A, Nainu F, Arba M, Paneo DR, Praditapuspa EN, Maulana S. Network Pharmacology and Molecular Docking Studies of Ethnopharmacological Plants from Sulawesi as Antidiabetics. Trop J Nat Prod Res. 2025; 9(3):1123–1135.
14. Baroroh, S.Si., M.Biotek. U, Muscifa ZS, Destiarani W, Rohmatullah FG, Yusuf M. Molecular interaction analysis and visualization of protein-ligand docking using Biovia Discovery Studio Visualizer. Indo J Comput Biol (IJCB). 2023; 2(1):22-30.
15. Paat VI, Aloanis AA, Maya J, Najoan J. Molecular Docking Of Cyclosenegalin A As Anticancer. Fuller Chem J. 2025; 10(1):26–33.
16. Li X, Xin Y, Mo Y, Marozik P, He T, Guo H. The Bioavailability and Biological Activities of Phytosterols as Modulators of Cholesterol Metabolism. Molecules. 2022; 27(523):1–15.
17. Tuj Johra F, Kumar Bepari A, Tabassum Bristy A, Mahmud Reza H. A mechanistic review of β-carotene, lutein, and zeaxanthin in eye health and disease. Antioxidants. 2020; 9(11):1–21.
18. Md Idris MH, Mohd Amin SN, Mohd Amin SN, Nyokat N, Khong HY, Selvaraj M, Zakaria ZA, Shaameri Z, Hamzah AS, Teh LK, Salleh MZ. Flavonoids as dual inhibitors of cyclooxygenase-2 (COX-2) and 5-lipoxygenase (5-LOX): molecular docking and in vitro studies. Beni Suef Univ J Basic Appl Sci. 2022; 11(117):1–9.
19. Ahmadi M, Bekeschus S, Weltmann KD, von Woedtke T, Wende K. Non-steroidal anti-inflammatory drugs: recent advances in the use of synthetic COX-2 inhibitors. RSC Med Chem. 2022; 13(5):471–496.
20. Musfiroh I, Kartasasmita RE, Ibrahim S, Muchtaridi M, Hidayat S, Ikram NKK. Stability Analysis of the Asiatic Acid-COX-2 Complex Using 100 ns Molecular Dynamic Simulations and Its Selectivity against COX-2 as a Potential Anti-Inflammatory Candidate. Molecules. 2023; 28(9):1–11.
21. Desantis F, Miotto M, Di Rienzo L, Milanetti E, Ruocco G. Spatial organization of hydrophobic and charged residues affects protein thermal stability and binding affinity. Sci Rep. 2022; 12(1):1–13.
22. Al-Mughram MH, Catalano C, Herrington NB, Safo MK, Kellogg GE. 3D interaction homology: The hydrophobic residues alanine, isoleucine, leucine, proline and valine play different structural roles in soluble and membrane proteins. Front Mol Biosci. 2023; 10(1):1–24.
23. Singh CD, Kumar Gupta A, Deepak M, Chaudhary S. Silico and Analytical Evaluation of Beta-Sitosterol From *Anogeissus Pendula* As A Potential Therapeutic Agent Against Hyperlipidemia. J Neonatal Surg ISSN [Internet]. 2025; 2(1):12–16. Available from: https://www.jneonatalsurg.com
24. Owoloye AJ, Ligali FC, Enejoh OA, Musa AZ, Aina O, Idowu ET, Oyebola KM. Molecular docking, simulation and binding free energy analysis of small molecules as Pf HT1 inhibitors. PLoS One. 2022; 17(8):1–18.
25. Naznin NE, Mazumder T, Reza MS, Jafrin S, Alshahrani SM, Alqahtani AM, Shahid Ud Daula AFM. Molecular Docking Supported Investigation of Antioxidant, Analgesic and Diuretic Effects of *Costus Specious* Rhizome. Bull Chem Soc Ethiop. 2022;36(3):627–640.
26. Ma LS, Jia XT, Hu FQ, Zheng YJ, Huang XF, Rausch-Fan X, Fan XC. Mechanism of *Lycium barbarum* in treating periodontitis based on network pharmacology, molecular docking, and experimental validation. Clin Oral Investig. 2025; 29(219):1–14.
27. Muzyamba S, Singh I Sen. GC-MS, GNPS and METLIN Assisted Phytochemical Profiling, Bioactivity Study and Molecular Docking Analysis of *Paropsia brazzeana* Root Bark, a Medicinal Plant in Zambia. Sys Rev Pharm [Internet]. 2024; 15(1):1–14. Available from: https://www.researchgate.net/publication/378549828
28. Adelia M, Setiawansyah A, Sitindaon RS. Potential activity of *Stevia rebaudiana Bert*. in Inhibiting Cyclooxygenase and Lipooxygenase Enzymes as Anti-inflammatory Candidates: A Molecular Docking Study and ADMET Prediction. J Drug Deliv Ther. 2023; 13(7):75–86.
29. Oladoja FA, Awodele O, Oreagba IA, Irokosu ES, Oyinloye EO, Murtala AA. Anti-inflammatory activity and molecular docking studies of the hydromethanolic leaf extract of *Baphia longipedicellata brumitt* in rats. Pharmacol Res - Mod Chin Med. 2024; 13(2024):1–9.
30. Jain S, Ganeshpurkar A, Dubey N. Molecular Docking of some Neem Constituents with COX-2 and NOs: An in silico Study. Pharmacogn Commun. 2020; 10(3):134–135.
31. Utami W, Aziz HA, Nasrudin D, Kusmawan A, Anwar Z, Maulana M, Daryanto M. Investigating the potency of bioactive compounds from *Ficus religiosa* as anti-inflammatory agent. J Phys Conf Ser. 2021; 1869(2021):1–6.
32. Akinloye OA, Akinloye DI, Onigbinde SB, Metibemu DS. Phytosterols demonstrate selective inhibition of COX-2: In-vivo and in-silico studies of *Nicotiana tabacum*. Bioorg Chem. 2020; 102(2020):1–13.

33. Zhang G, Qi X, He L, Wang X, Zhao Y, Wang Q, Han J, Wang Z, Ding Z, Liu M. Non-covalent complexes of different pH levels: Binding interactions, storage stabilities, and bioaccessibilities. Curr Res Food Sci. 2024; 8(2024):1–10.
34. Shi G, Gu L, Jung H, Chung WJ, Koo S. Apocarotenals of Phenolic Carotenoids for Superior Antioxidant Activities. ACS Omega. 2021; 6(38):25096–25108.
35. Jafari Z, Bigham A, Sadeghi S, Dehdashti SM, Rabiee N, Abedivash A, Bagherzadeh M, Nasseri B, Karimi-Maleh H, Sharifi E, Varma RS, Makvandi P. Nanotechnology-Abetted Astaxanthin Formulations in Multimodel Therapeutic and Biomedical Applications. J Med Chem. 2022; 65(1):2–36.
36. Sadoud M, Zidane A, Metlef S, Nemar F, Riazi A. The properties of astaxanthin extracted from Algerian green microalga *Haematococcus pluvialis.* Afr J Biol Sci [Internet]. 2024; 6(15):9583–9599. Available from: https://doi.org/10.48047/AFJBS.6.15.2024.9582-9599
37. Akinade TC, Babatunde OO, Adedara AO, Adeyemi OE, Otenaike TA, Ashaolu OP, Johnson TA, Terriente-Felix A, Whitworth AJ, Abolaji AO. Protective capacity of carotenoid trans-astaxanthin in rotenone-induced toxicity in *Drosophila melanogaster*. Sci Rep. 2022; 12(1):1–13.
38. Liu Z, Li Y, Bao J, Li S, Wen Y, Zhang P, Feng J, Wang Y, Tian L, Jie Y. Astaxanthin ameliorates benzalkonium chloride–induced dry eye disease through suppressing inflammation and oxidative stress via Keap1-Nrf2/HO-1 signaling pathways. Animal Model Exp Med. 2025; 6;1–24.
lutein/zeaxanthin and whey protein isolate formed at
39. Yang S, Lin X, Shi B, Meng J, Liu L, Yan L, Xie F. Hydrastinine and β-sitosterol Synergistically Target Acute Myelocytic Leukemia in a Ferroptosis-Related Prognostic Model. Res Sq [Internet]. 2023; 1–25. Available from: https://www.researchsquare.com/article/rs-3770830/v1
40. Shinde P, Singh G, Kardile D, Salunke M, Kashid S. Beta-Sitosterol and Stigmasterol as Synergestic Anticancer Potential in Breast Cancer Isolated from *Euphorbiaceae* Family Plants. Afr J Biomed Res [Internet]. 2024; 27(4):1929–1934. Available from: https://africanjournalofbiomedicalresearch.com/index.php/AJBR/article/view/3966
41. Cai L, Cai Y, Yu R, Song A, Yang C, Yang W, Jiang F. Synergistic Analgesic Effects of Astaxanthin Combined with Celecoxib on a Mouse 2 Bone Cancer Pain Model: From Behavioral Validation to Target Prediction. SSRN [Internet]. 2025; 1–48. Available from: https://ssrn.com/abstract=5243617
42. Marzagalli M, Battaglia S, Raimondi M, Fontana F, Cozzi M, Ranieri FR, Sacchi R, Curti V, Limonta P. Anti-Inflammatory and Antioxidant Properties of a New Mixture of Vitamin C, Collagen Peptides, Resveratrol, and Astaxanthin in Tenocytes: Molecular Basis for Future Applications in Tendinopathies. Mediators Inflamm. 2024; 5273198 1–17.